JOURNAL OF CHEMICAL INFORMATION AND MODELING

Article

pubs.acs.org/jcim

Structure-Based Virtual Screening and Biological Evaluation of a Calpain Inhibitor for Prevention of Selenite-Induced Cataractogenesis in an in Vitro System

Arumugam Ramachandran Muralidharan,[†] Chandrabose Selvaraj,[‡] Sanjeev Kumar Singh,[‡] Joen-Rong Sheu,[§] Philip A. Thomas,[∥] and Pitchairaj Geraldine*[,†]

[†]Department of Animal Science, School of Life Sciences, Bharathidasan University, Tiruchirappalli−620024, Tamilnadu, India

[‡]Department of Bioinformatics, Alagappa University, Karaikudi−630003, Tamilnadu, India

[§]Graduate Institute of Medical Sciences, College of Medicine, Taipei Medical University, Taipei 110, Taiwan

[∥]Institute of Ophthalmology, Joseph Eye Hospital, Tiruchirappalli−620001, Tamilnadu, India

ABSTRACT: Calpains belong to the family of calcium-dependent, structurally related intracellular cysteine proteases that exhibit significant functions in evolution of different types of cataracts in human as well as animal models. Application of calpain inhibitors generated through a virtual screening workflow may provide new avenues for the prevention of cataractogenesis. Hence, in the current study, compounds were first screened for potent calpain inhibitory activity by employing a structure-based approach, and the screening results were then validated through biological experiments in rat lenses. A hit compound, HTS08688, was obtained by structure-based virtual screening. A micromolar concentration of HTS08688 was found to prevent in vitro cataractogenesis in isolated Wistar rat lenses, while maintaining the antioxidant and calcium concentrations at near normal levels. Inhibition of superoxide anion generation, as observed through cytochemical localization studies, and maintenance of structural integrity, as demonstrated by histological analysis of lenticular tissue, also suggested that HTS08688 can ameliorate the cataractous condition induced by selenite in an in vitro rodent model. A cell proliferation assay was performed; the IC 50 value of the screened calpain inhibitor, HTS08688, against human lenticular epithelial cells-b3 was found to be 177 μM/mL. This combined theoretical and experimental approach has demonstrated a potent lead compound, HTS08688, that exhibits putative anticataractogenic activity by virtue of its potential to inhibit calpain.

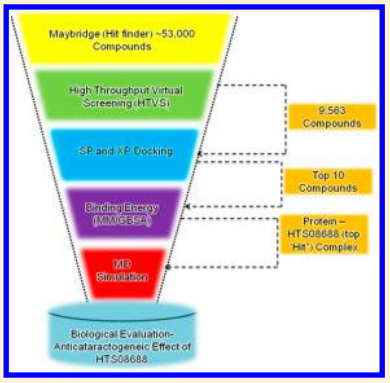

INTRODUCTION

Cataracts, which are characterized by loss of transparency of the crystalline lens, are the commonest global etiology of preventable blindness.[1] Cataract formation is principally an age-related occurrence, although social, economic, and lifestyle factors may also contribute to its prevalence. Currently, surgical removal of the cataractous lens is the preferred therapeutic modality for cataract. However, the demand for highly trained personnel and the cost of surgery pose a significant economic problem. Thus, the need for preventing or delaying the progression of cataract formation by an alternative therapeutic modality is essential. Excessive production of free radicals and reactive oxygen species (ROS) leading to oxidative damage has been recognized as one of the key factors inducing human senile cataract formation. Free radicals, perturbing the ionic homeostasis of the lens, have been reported to cause loss of transparency.[2]

Intracellular free calcium (Ca^{2+}) has been recognized to play a central role as a second "messenger" in numerous cellular events through myriad of specialized regulatory as well as signaling proteins; elevated Ca^{2+} has also been reported to elicit pathological events in cell death.[3,4] The lens is no exception to these cellular functions; total Ca^{2+}in human cataractous lenses was reported to be 3000-fold higher than that in normal human lenses.[5] The opacification of the human lens is primarily due to the imbalance in Ca^{2+} homeostasis that initiates a cascade of molecular events: these include oxidation of critical sulfhydryl groups of Ca^{2+}-ATPase within the lenticular epithelial membrane, entry of Ca^{2+} from the anterior chamber fluid and the subsequent activation of the cysteine protease, calpain, which is followed by truncation of the N- and C-terminal extension in crystallins, thereby resulting in interplay among the free charged groups.[6]

Calpains belong to the superfamily of Ca^{2+}-dependent structurally homologous intracellular cysteine proteases.[7,8] Although their precise physiological function remains poorly defined, calpains appear to participate in various cellular mechanisms.[9]

Localized pathological elevation of intracellular Ca^{2+} has been found to result in activation of calpains, thereby triggering several human disorders, including cataract.[10,11] Five different calpain isoforms occur in lenticular tissue; these include calpain 1 (μ calpain), calpain 2 (m calpain), calpain 10, and the

Received: February 17, 2015
Published: August 13, 2015

DOI: 10.1021/acs.jcim.5b00092
J. Chem. Inf. Model. 2015, 55, 1686−1697

lenticular-specific calpains, namely, Lp82 and Lp85. Cataractogenesis occurs to the accompaniment of putative biochemical indicators of calpain activation, such as increased lenticular calcium levels, proteolysis of α-spectrin, and reduced caseinolytic activity toward calpains, suggesting possible calpain activation and subsequent autolysis.[12] Some investigators have reported that activation of calpain causes disintegration of lenticular proteins involved in maintenance of functional and structural integrity, resulting in opacification of the lens in experimental models.[13,14] The experimental rodent model of selenite cataract mimics human senile cataract in several aspects including raised levels of Ca^{2+} and insoluble protein, accelerated proteolytic activity and reduced levels of aqueous-soluble protein as well as reduced glutathione (GSH).[6] Selenite cataract serves as an extremely rapid and favorable model of senile nuclear cataract. The reproducibility and acceptability of the selenite-induced rodent cataract make this an effective experimental model to quickly screen molecules for putative anticataractogenic effects.

Several experimental studies have demonstrated that inhibitors of calpain may inhibit lenticular calpain activity, thereby preventing or retarding cataractogenesis.[15,16] Although several calpain inhibitors have been identified, both from natural products and through chemical synthesis,[17] most of these have low metabolic stability, and poor membrane permeability and selectivity.[18]

In the present investigation, an effective strategy to screen potential calpain inhibitors through a high throughput virtual screening (HTVS) approach was adopted, employing the HTVS platform available in the Schrödinger suite (Schrödinger LLC, New York, USA), in an attempt to maximize possible pharmaceutical potential of the inhibitors. Prior to virtual screening, the ligands available with Maybridge (Thermo Fisher Scientific Inc., LE, UK) were subjected to absorption, distribution, metabolism and excretion (ADME) calculations, followed by filtration through the "Lipinski rule of five". In order to validate the final hit compound, the mutated (S115C) calpain 1 (1KXR)−ligand complex was subjected to molecular dynamics simulation. Subsequently, experimental validation of the anticataractogenic property of the "hit" compound was determined in an in vitro experimental animal model of sodium selenite-induced cataract.

MATERIALS AND METHODS

Computational Analysis. *System Specification.* The entire in silico phase of the study was done using a High Performance Cluster (HPC) function with the Cent OS V6.2. Hardware configuration of the HPC cluster was Locuz cluster-Super micro SC826TQ-R1200 LIB series, with 2 ATOM processor of 32 Core and 32 GB RAM speed. To perform molecular modeling studies, a commercial version of Schrödinger software package[19] was used. Molecular dynamics simulation was performed employing an academic module of Desmond V.3.7 molecular dynamics package.

Protein Preparation and Structure Refinement. X-ray crystallographic structural details of the calcium-bound protease core of calpain 1 (1KXR)[20] with a resolution of 2.07 Å was retrieved from the Protein Data Bank (PDB).[21] Additional preparation was done using the Protein Preparation Wizard of the Schrödinger Suite[22,23] to ensure that the downloaded X-ray structure was reliable and qualitatively considerable for further in silico studies; this preparation also removes potentially occurring stereochemical short contacts in the protein structure by optimization and minimization protocols. Prior to protein preparation, the Ser115 residue of 1KXR was mutated to Cys115, so as to mimic the protein in physiological conditions; this was done using the standard mutation protocol of the Schrödinger software.[16,24] Chemical accuracy was ensured by addition of hydrogen atoms, correcting the bond orders and by neutralizing the side-chains which were neither close to the binding cavity nor were involved in the construction of salt bridges. The structure prepared underwent minimization by adopting the Protein Preparation Wizard with optimal potential to create the liquid simulation (OPLS)-2005 force field (FF) at an intermediate docking stage. The subsequent step involved removal of water molecules without any contact and addition of hydrogen atoms to the structure, principally at the sites of the hydroxyl and thiol hydrogen atoms, to correct ionization as well as tautomeric states of the amino acid residues. The residues occurring within a distance of 5 Å from the calcium ions on the crystal structure were maintained in a frozen state during this minimization.[25,26] In addition to the protein optimization step, the Cys115 was also deprotonated as reported earlier by Muralidharan et al.[24] The optimized model structure was minimized until the average root-mean-square deviation (RMSD) of the non-hydrogen atoms reached 0.30 Å using the OPLS- all atom (AA) force field.

Active Site Prediction. Although the residues Cys 115, Asn 272, and His 296 of the calpain 1 protein were constituted to form a catalytic triad in physiological conditions, additional residues that constituted the binding pocket for the modeled structure were also determined to accentuate the discovery of the new lead. For this, predictions of putative interacting residues were made through Sitemap with OPLS-2005.[27,28] Sitemap provides an indication about the positions that are suitable for a donor or acceptor or about the hydrophobic group that needs to occur in the receptor. The druggability regions were delineated using physical descriptors such as size, degree of enclosure or exposure, extent of tightness, hydrophobicity, hydrophilicity, possibilities of hydrogen-bonding and binding site points probably contributing to protein−ligand binding.

High Throughput Virtual Screening. A "standalone" library comprising approximately 53 000 drug-like compounds of the Maybridge database was prepared by using OPLS 2005 FF. 3D structures of the small molecules were prepared by using LigPrep prior to docking simulation so as to obtain the accessible least-energy ionized conformer and tautomeric states of the ligands.[29] This was then kept for Virtual Screening Workflow (VSW). In VSW, the compounds were subjected to ADME property calculation using Qikprop module.[30] ADME descriptors are usually calculated at the terminal stage of the drug discovery protocol; however, in the present investigation, we performed the ADME property calculation in the preliminary stages of drug development to permit identification and elimination of false-positive molecules with poor pharmacokinetic characteristics in the preliminary phases of the drug discovery pipeline, thereby ensuring significant cost savings. The program was executed by employing a default mode for the principal descriptors and physicochemical properties of all Maybridge compounds, with detailed analysis of the $\log^{P}$ (octanol/water), $Q^{P}\log^{S}$ (the predicted aqueous solubility), $Q^{P}\log^{BB}$ (the predicted partition coefficient of the brain/blood barrier), and percentage of human oral absorption. In addition, QikProp assessed the suitability of all Maybridge compounds based on Lipinski's rule of 5.[31] In silico screening

DOI: 10.1021/acs.jcim.5b00092
J. Chem. Inf. Model. 2015, 55, 1686−1697

was performed in the VSW, to detect ligands that were likely to interact with druggability sites of the mutated 1KXR protein configuration. The ligands thus prepared were docked against the druggability pocket over which the grid had been generated. The high throughput virtual screening (HTVS), standard precision (SP) and extra precision (XP) module of Glide was assigned with default values.[32,33] Top hit compounds were ranked based on the Glide score. A docking-based screening protocol was implemented stepwise and, at the end of each step, compounds possessing a score higher than that of the cutoff were chosen for the next step.[32] During the docking process, the Glide scoring function (G-score) was employed to identify the best conformation for each ligand. Finally, Glide energy was calculated using the Glide score and a single best pose was obtained as output for a specific ligand.

Free Energy Calculation. Binding energy calculations are termed to be accurate when compared to docking energy calculations.[34] Therefore, in the present investigation, the MM/GBSA algorithm in the Prime module of the Schrödinger Suite was employed to determine the binding energy. The binding energy was calculated by the following equation:

$$\Delta G_{\text{bind}} = \Delta_{\text{E}} + \Delta G_{\text{solv}} + \Delta G_{\text{SA}}$$

where, $\Delta_{\text{E}} = E_{\text{complex}} - E_{\text{protein}} - E_{\text{ligand}}$, the E_{complex}, E_{protein}, and E_{ligand} denoting the minimized energy values of, respectively, the protein−ligand complex, protein only, and inhibitor only. The electrostatic solvation energy of the complex has been represented as ΔG_{solv}. Similarly, the nonpolar contribution by the surface area to the solvation energy has been represented as ΔG_{SA}.

Molecular Dynamics (MD) Simulations. MD simulations were employed to obtain the most stable conformation of calpain mutant and conformational changes with inhibitor complexes, the binding influence of the screened inhibitor with mutant calpain and also to understand the protein−ligand interactions in a dynamic state. The Desmond program package[35] was used for MD simulations adopting the OPLS-AA FF parameter. To perform MD simulation studies, solvation of structures was done by a three site (TIP3P) water model, the solvated structures being energy-minimized by the steepest descent method and ending following maximum force being obtained in smaller than 100 kJ/mol·nm.[36] The apoprotein, protein−ligand complex underwent energy-minimization utilizing Desmond with OPLS-AA force field parameters. Prior to thermalisation, all systems underwent up to 100 steepest descent energy minimization steps, for a maximum force exceeding 100 kJ/mol·nm. After thermalization, MD simulation was run at the isothermal−isobaric (NPT) ensemble at a constant temperature of 300 K and pressure of 1 bar, with a time step of 2 fs and application of the relaxation time between 0.1 and 0.4 fs.[33] Simulation of the canonical ensemble moles (N), volume (V), and temperature (T) was carried out for 1 ns and equilibration of the simulated conformers was done for 10 ns of the time scale.

Experimental Analysis. *In Vitro Experiments on Rat Lenses.* Animal experiments were conducted per Institutional guidelines (Reference No. of Institutional Ethical Committee approval: BDU/IAEC/2012/57/28.03.2012) and protocols approved by the Association for Research in Vision and Ophthalmology Statement for the Use of Animals in Research. Diethyl ether was used to anesthetize Wistar rats weighing 75−90 g, which were then killed by cervical dislocation. Lenses were removed immediately and immersed in Dulbecco's modified Eagle's medium (DMEM, Gibco, Life Technologies, USA) containing streptomycin (60 μg/mL) and penicillin (60 μg/mL) to prevent bacterial contamination. After 2 h, only transparent undamaged lenses were assigned to three specific groups:

1. Group I (n = 8) which consisted of lenses cultured in DMEM alone (normal [control])
2. Group II (n = 8) which consisted of lenses cultured in DMEM containing 100 μM/mL sodium selenite (Sigma-Aldrich, St. Louis, MO, USA) (selenite-challenged, untreated)
3. Group III (n = 8) which consisted of lenses cultured in DMEM containing 100 μM/mL sodium selenite and 100 μM/mL of the in silico-screened calpain inhibitor (selenite-challenged, HTS08688-treated)

These lenses were maintained for 24 h at 37 °C in cell culture test plates placed in an incubator with 5% CO_2. At the end of the 24 h, the lenses first underwent gross morphological examination followed by processing to permit subsequent biochemical and other analyses.

Gross Examination of Lenticular Morphology. A dissecting microscope was used to magnify the lenses with black gridlines in the background. Opacities were delineated as follows:

(a) 0, indicating absence of opacification (gridlines sharp and clear)
(b) +, indicating minimal opacification (slight clouding of gridlines [gridlines still clear])
(c) ++, indicating definite diffuse opacification of almost the entire lens (moderate clouding of gridlines [gridlines neither clear nor sharp])
(d) +++, indicating widespread thick opacification of the entire lens (total clouding of gridlines [gridlines not visible])

Preparation of Lens for Biochemical Analysis. After morphological examination and before biochemical analysis was performed, lenses taken from each of the groups were washed in 0.85% saline and weighed. Each lens underwent homogenization in a volume of 50 mM phosphate buffer (pH 7.2) that was 10-fold its mass and centrifuged at 12 000g for 15 min at 4 °C. Biochemical analysis was performed on the resulting supernatant. The concentration of protein in each sample was measured by the method of Bradford,[37] with bovine serum albumin serving as a standard.

Measurement of Activities of Enzymatic Antioxidants in Supernatant from Lenticular Homogenate. Superoxide dismutase (SOD) activity (expressed as unit/min·mg protein) was assayed by a standard method[38] that involves measuring the extent to which pyrogallol auto-oxidation is inhibited by the supernatant of the lenticular homogenate; variations in absorbance at 470 nm were detected by spectrophotometry against a blank every minute for 3 min.

The activity of catalase (CAT) (noted as millimoles of hydrogen peroxide [H_2O_2] utilized/min·mg protein) was determined essentially as detailed by Sinha,[39] wherein when dichromatic acetic acid is heated along with H_2O_2, it is reduced to chromic acetate, with perchloric acid formed as an intermediate of poor stability. The resulting green color was read by spectrophotometry against a blank.

Glutathione peroxidase (Gpx) activity (noted as micromole of glutathione oxidized/min·mg protein) was measured by a standard method,[40] wherein the rate at which H_2O_2 oxidize glutathione (with Gpx in the supernatant serving as a catalyst)

DOI: 10.1021/acs.jcim.5b00092
J. Chem. Inf. Model. 2015, 55, 1686−1697

is measured, the color that develops being read spectrophotometrically at 412 nm against a reagent blank.

Measurement of GSH Concentration in Supernatant from Lenticular Homogenate. The concentration of GSH (μmol/g wet weight of the lens), a nonenzymatic antioxidant, was determined by the procedure of Moron et al.[41] Homogenization of each lens was done in 1.0 mL of 0.1 M phosphate buffer, followed by centrifugation at 2000*g* for 15 min at 4 °C. To the resulting supernate of the lenticular homogenate, 10% trichloroacetic acid (0.5 mL) was added, followed by recentrifugation of the mix. A 4 mL portion of 0.3-M Na_2HPO_4 (pH 8.0) and 0.5 mL of 0.04% (w/v) 5,5-dithiobis-2-nitrobenzoic acid were then added to the resulting protein free supernate. A yellow color developed, the absorbance of which was read spectrophotometrically at 412 nm. The results were noted as micromoles per gram wet weight of the lens.

Determination of Lipid Peroxidation. The concentration of malondialdehyde (MDA), a measure of lipid peroxidation, was determined by measuring thiobarbituric acid-reacting substances (TBARS) by a reference method.[42] For this assay, lenses were homogenized in 0.15 M potassium chloride (1.0 mL). In a reaction tube, 8.1% sodium dodecyl sulfate (0.2 mL), 20% acetic acid (1.5 mL, pH 3.5), and 0.81% thiobarbituric acid aqueous solution (1.5 mL) were added in succession to prepare a reaction mixture to which 0.2 mL of the lenticular homogenate was added. Heating of the mixture in boiling water was done for 60 min followed by cooling to room temperature and addition of 5 mL of butanol:pyridine (15:1 v/v) solution. This mixture was centrifuged at 2000*g* for 15 min following which the upper organic layer was aspirated. The intensity of the resulting pink color was read at 532 nm with tetramethoxypropane being used as an external standard. The concentration of lipid peroxides was noted as nanomole of MDA generated per gram wet weight of lens.

Detection of Nitroblue Tetrazolium-Reducing Substances in Whole Lenses by a Cytochemical Method. Cytochemical detection of O_2^- generated in Wistar rat pup lenses was done by the nitroblue tetrazolium (NBT) reduction method.[43] Briefly, each entire (whole) lens was incubated at 22 °C for 1 h with 100 μL of 0.3% NBT and, then, washed with Tris-HCl buffer (pH 7.4, 0.1 M Tris). Using a Carl Zeiss Axiolab (Oberkochan, Germany) microscope, blue formazan deposits were sought under bright-field optics (total magnification 5×)

Measurement of Calcium Concentration in Lenses. To measure lenticular calcium concentration, the lenses were first heated at 100 °C for 20 h followed by determination of their dry weight. Digestion of the lenses with 0.2 mL concentrated HCl was done at room temperature overnight, followed by adjustment to 1.0 mL with deionized water. Centrifugation of the resulting mixtures at 10 000*g* was done for 10 min to remove insoluble material, if any. Measurement of the calcium concentrations in the supernatant (μmol of calcium/g dry weight of lens) was performed by an atomic absorption spectrophotometer (model Spectra AA-220 FS, Varian, Australia), which was operated at a wavelength of 422.7 nm and a 0.5 nm wide slit. Standard solutions were prepared from calcium carbonate and deionized water.

Calpain Activity Assay. Using casein as a substrate, the combined activity of calpains was measured fluorimetrically by a standard method,[44] with minor modifications. From each group, rat lenses underwent comprehensive homogenization in 10 vol of 10 mM sodium borate buffer, pH 8.0, containing 5 mM ethylenediaminetetracetic acid (EDTA), 3 mM sodium azide, 1 mM dithiothreitol, and 0.1% Triton X-100. The homogenate was then centrifuged at 10,000g for 10 min and calpain activity was measured in the resulting supernatant. The substrate was prepared by boiling an aqueous solution of casein (60 mg/mL) at pH 9.5 (maintained by addition of 0.1 N NaOH [20 μL]), followed by cooling, titration to pH 5.9 using 0.1 N HCl, and centrifugation to yield a supernate. Defined volumes of lenticular homogenate (containing approximately 500 μg of protein) were added to a mixture containing 3.57 mg of alkali-treated casein, 25 mM of sodium borate, 1 mM of 2-mercaptoethanol, and 5 mM of $CaCl_2$ up to a total volume of 0.35 mL. The resulting incubation mixture had a pH of 7.5, and this was incubated for 1 h at room temperature (incubation mixture without calcium contained 1 mM ethylene glycol tetraacetic acid [EGTA]). Zero-time incubation blanks were subtracted. The enzyme reaction was terminated on addition of 200 μL of 36% (w/v) trichloroacetic acid, following which the tubes were maintained at 4 °C overnight. Following centrifugation, 200 μL of trichloroacetic acid supernate were mixed with 1.5 mL of 0.1 M sodium borate buffer (pH 8.5) and 200 μL fluorescamine solutions (3.4 mg/10 mL of acetone) were added to each tube; the contents were then mixed thoroughly. The quantum of liberated amino groups was measured fluorimetrically[45] in a spectrofluorimeter and compared with standards of known amounts of glutamate in 10% trichloroacetic acid. One unit of calpain activity was defined as the amount that caused the release of 1 μmol of amino groups/h under the conditions described. Results were denoted as micromoles of glutamic acid equivalents released per milligram protein per hour.

Histological Study of Lens. Fixation of the lenses was done for 2 h at room temperature in Sorenson's buffer (88% Sorenson's sodium phosphate buffer, 3% glutaraldehyde, and 9% deionized water). The lenses were processed in a graded series of ethanol and then infiltrated and embedded in paraffin wax at 57 °C. Infiltration occurred over 72 h at 4 °C on a low shaker with daily changes of solution.[46] Sections (5 μm thickness) were sliced using a tungsten carbide knife on a Leica RM 2055 rotary microtome, placed on glass slides and incubated overnight at 60 °C; these were then stained with hematoxylin and alcoholic eosin. The stained sections were examined by bright-field microscopy (Carl Zeiss Axioskop 2 plus; Jena, Gera, Germany).

Culture of Lenticular Epithelial Cells. Human lenticular epithelial B3 (HLE-B3) cells were a kind gift from Dr. Sridhar Rao (Centre for Cellular and Molecular Biology, Hyderabad, India). HLE-B3 cells were cultured in Eagle's minimum essential medium (MEM; Invitrogen- Gibco, Grand Island, NY, USA) supplemented with 20% fetal bovine serum (FBS; Invitrogen-Gibco) and 50 μg/mL gentamicin (Invitrogen-Gibco) at 37 °C in a humidified 5% CO_2 atmosphere.

Assay of Lenticular Epithelial Cell Proliferation. The proliferation of HLE-B3 cells was examined by a colorimetric 3-4,5-(dimethyl-thyazol-2-yl)-2,5-diphenyltetrazolium (MTT) (Sigma- Aldrich) assay. In brief, the cells were cultured as described earlier, except that the cells were seeded in 96-well tissue culture plates at a density of 5×10^3 cells/well. The cells were treated with 0.5 mg/mL of the MTT labeling reagent and incubated at 37 °C for 1 h. A dark blue formazan product of MTT was extracted by the MTT lysing solution (40 mM HCl in isopropyl alcohol) and measured (absorbance of 570 nm) by

DOI: 10.1021/acs.jcim.5b00092
J. Chem. Inf. Model. 2015, 55, 1686−1697

an automatic ELISA reader (SpectraMax 250; Molecular Devices, Sunnyvale, CA).

Statistical Analysis. Statistical analysis was carried out using the Statistical Package for Social Sciences (SPSS) software package for Windows platform (Version 16.0; IBM Corporation, Armonk, NY). Differences between all experimental groups were sought by one-way analysis of variance (ANOVA). Posthoc testing was done to allow intergroup comparisons using the least significance difference test. The chi-square test was applied wherever relevant. P values <0.05 were considered statistically significant.

RESULTS AND DISCUSSION

Structural Refinement of Protein. Calpain 2 was identified as the predominant calpain in human lenticluar epithelial cells that exhibited age-related cortical cataract[47] and also reported to be involved in rodent lenticular opacification.[48] Although calpain 1 is expressed at only minimal levels in the lens, it shares a high degree of sequence homology and structural organization exhibiting dimeric topology with a catalytic subunit made up of domains I–IV, as well as a regulatory subunit comprising domains V and VI. Moldoveanu et al.[49] found that the structural determinants for Ca^{2+}-dependence were conserved among the calpain isoforms. Ca^{2+}-bound calpain 1 has been found to serve as an ideal drug target for design and validation of inhibitors targeted toward the active site pockets. Hence, in the present investigation, the crystal structure of calpain was employed to identify potent and specific inhibitors. The Ser 115 residue of calpain was mutated to Cys 115 so as to mimic the binding mode of the native protein occurring in the physiological state, thereby facilitating the realignment and assembling of domains IIa and IIb, which possessed the binding site residues. The stereochemical and overall quality factor of the energy-minimized structure was found to be satisfactory; the resulting model was employed in the subsequent screening (Figure 1).

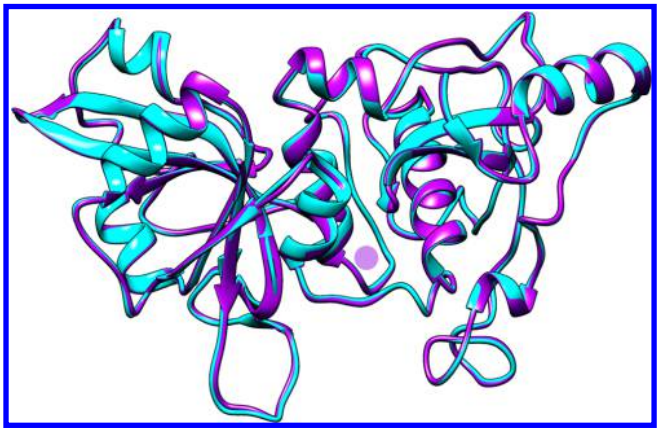

Figure 1. Superimposed protein structure of calpain 1 (1KXR) with colors, cyan indicating the wild type and violet indicating the mutated structure of 1KXR. Blue sphere indicates the site of mutation (SER115 to CYS115).

The amino acid residues Ile 25, Gly 113, Cys 115, Trp 116, Ser 206, Gly 207, Gly 208, Cys 209, Thr 210, Ser 251, Asn 253, Asp 256, Ile 257, Asp 259, Leu 260, Glu 261, Ala 262, Arg 270, Gly 271, His 272, and Ala 273, that were predicted to form the binding pocket, are consistent with the active site residues that were experimentally proven and additionally corroborate the results generated recently by Muralidharan et al.[24]

Molecular Docking and Virtual Screening. Shoichet[50] and Cheng et al.[51] emphasized the significance of virtual screening over high-throughput screening, a conventional technology in practice at most pharmaceutical industries. Ghosh et al.[52] compiled the success rate of receptor-based virtual screening on various targets, including proteases. Although Muralidharan et al.[24] performed ligand-based virtual screening to identify inhibitors for calpain 1, those screened inhibitors were reported to possess the features of already-established inhibitors. The structure-based virtual screening methodology remains highly desirable for identification of novel compounds with structural diversity since the active site of the calpain protein serves as a target.

In the present investigation, drug-like Maybridge compounds optimized with the OPLS-2005 force field were subjected to ADME filters so as to reduce false-positives and to avoid molecules possessing poor pharmacokinetic profiles. Significant ADME parameters thus calculated were octanol/water partition coefficient (QPlogPo/w), water solubility (QPlogS), brain/blood partition coefficient (QPlogBB), and percentage human oral absorption. Corresponding cutoff values were allotted for the calculated ADME parameters, namely, QPlogPo/w, −3.5; QPlogS, −4.0; QPlogBB, −0.5; percentage human oral absorption, 70%. In addition, the Lipinski rule of five was also calculated with cutoff ranges designated to remove the outliers. As a result of these defined criteria, the standalone library was compressed to 9563 compounds, which was then subjected to a stepwise HTVS protocol. Initially, standard precision and extra-precision docking were carried out as illustrated by Stuart et al.,[16] in order to calculate the Glide score and Glide energy. Figure 2 depicts the 2D conformation of the ligands with the top ten highest scores obtained on using the HTVS protocol. *N*-[5-Ethyl-3-(4-methoxybenzoyl)-2-thienyl]-2-(4-methylpiperazino)acetamide (HTS08688), ethyl 4-{5-[4-(4-methylpiperazino)buta-1,3-dienyl]-2*H*-1,2,3,4-tetraazol-2-yl}benzoate (BTB12775) and *N*-(4-butyl-2-methylphenyl)-*N*′-

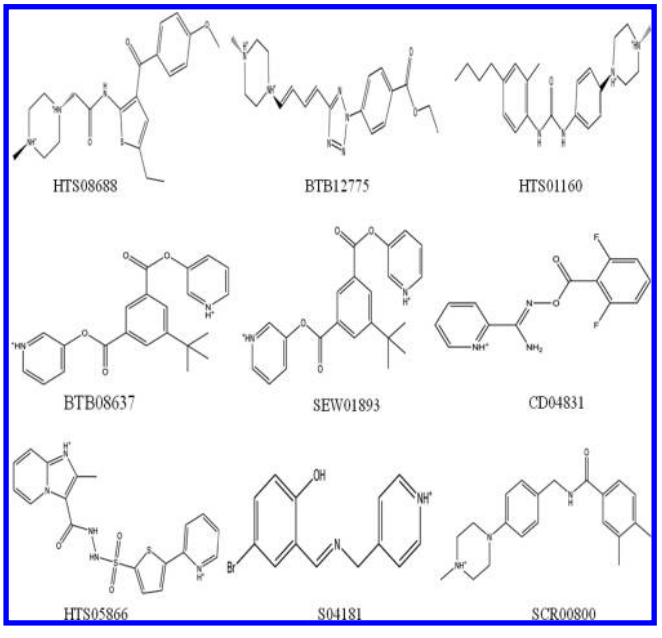

Figure 2. Two-dimensional conformations of selective "hit" compounds along with the corresponding Hitfinder ID.

DOI: 10.1021/acs.jcim.5b00092
J. Chem. Inf. Model. 2015, 55, 1686–1697

[4-(4-methylpiperazino)phenyl]urea (HTS01160) appeared to be the three key lead compounds, based on their Glide score and energy. Hydrogen-bond interactions were noted between the top three "hit" compounds and the active site residues (Figure 3). Of these compounds, HTS08688 showed the highest Glide score (−9.24 kcal/mol) and Glide energy (−57.74 kcal/mol) (Table 1), with five hydrogen bonds being formed with the binding pocket residues of calpain 1. The oxygen atom of the benzoyl group attached to the 4-methoxybenzoyl moiety of the ligand formed an hydrogen bond with the hydrogen of $-NH_2$ of Gln 109 (Lig:O_2···Gly 109, 2.4 Å); the second and third hydrogen bonds were formed between the oxygen atom of the methoxy group attached to the 4-methoxybenzoyl moiety of the ligand and $-NH_2$ of Cys 115 (Lig:O_2···Cys 115, 1.51 Å) and $-NH_2$ of Ala 273 (Lig:O_2···Ala 273, 2.49 Å), respectively. The fourth and fifth hydrogen bonds were formed between the oxygen atom of Glu 261 and, respectively, the hydrogen atom attached to the functional group acetamide (Glu 261···Lig:H, 1.65 Å), and the $-NH_2$ group attached to the 4-methylpiperazino group residing next to the chiral bond, which is considered to be optically active (Glu 261···Lig:H, 1.46 Å). Docking simulation demonstrated that BTB12775 exhibited the second highest Glide score (−9.2 kcal/mol) and Glide energy (−55.11 kcal/mol) (Table 1), with the formation of a single hydrogen bond between the oxygen atom of the ester group attached to the functional moeity benzoate of the ligand and the oxygen atom of Gly 208 present in the binding cavity of calpain 1. Compound HTS01160 demonstrated the formation of a single hydrogen bond between the oxygen atom of the functional moiety urea, and exhibited the third highest Glide score (−8.92 kcal/mol) and Glide energy (−52.9 kcal/mol). Interestingly, the present structure-based drug-designing approach revealed that the Glide scores (−9.24 kcal/mol, −9.2 kcal/mol and −8.92 kcal/mol) of the three lead compounds, namely HTS08688, BTB12775, and HTS01160, respectively, exceeded the scores of those inhibitors that had been screened through a ligand-based pharmacophore approach, the highest Glide score obtained there being −8.39 kcal/mol.[24] Furthermore, the Glide scores of the "hit" compounds derived in the present study were much higher than those of the Glide scores of already-established inhibitors, which includes SJA6017 and CAT 811 (exhibited a highest score of −6.45 kcal/mol) that were found to dock with the active site of calpain 1.[24] In the opinion of Perola et al.,[53] Glide score is a reliable scoring function for database screening, with consistent performance against pharmaceutically relevant protein−ligand complexes, especially, HIV-1 protease, inosine monophosphate dehydrogenase, and p38 MAP kinase. Further, Friesner et al.[32] confirmed the effectiveness of Glide Score to rank inhibitors by using different test sets of pharmaceutical importance which exhibited reproducible experimental binding affinity results. Hence, in the present study, we have ranked the inhibitors based on glide score. Powers et al.[54] hypothesized that the structure-based drug-designing approach would lead to the discovery of irreversible inhibitors against the protease family of enzymes, including cysteine proteases. The results of the present investigation, suggest that structure-based virtually screened compounds possess enhanced interaction with calpain 1, when compared to that exhibited by ligand-based-screened compounds.

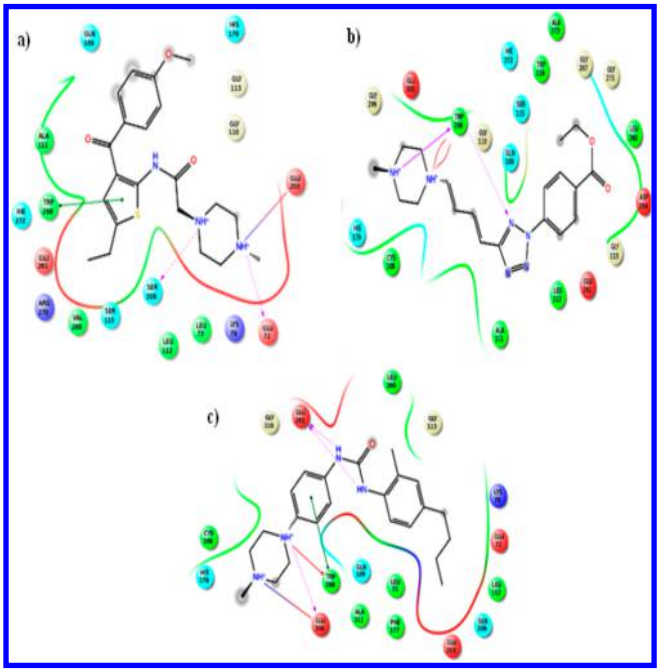

Figure 3. 2D interaction map of selective hits, (a) HTS08688, (b) BTB12775, and (c) HTS01160, obtained through the SBDD approach to the active site of calpain (1KXR).

Table 1. Docking Score and Energy Involvement of Hit Compounds against Calpain Employing a Structure-Based, Drug-Designing Approach

s. no.	Hitfinder ligand ID	G-score (kcal/mol)	Glide energy (kcal/mol)
1	HTS08688	−9.2366	−57.7405
2	BTB12775	−9.2002	−55.1068
3	HTS01160	−8.9212	−52.9039
4	BTB08637	−8.9037	−51.3070
5	SEW01893	−8.7189	−45.4976
6	CD04831	−8.6593	−40.5423
7	HTS05866	−8.6019	−55.3901
8	S04181	−8.4359	−42.7093
9	SCR00800	−8.4137	−43.1455
10	SCR00631	−8.3423	−55.8124

Binding Energy Calculation. The results of docking simulation were confirmed by determining the binding energy. The MM/GBSA score ascertained the binding efficiency of the hit compounds HTS08688, BTB12775, and HTS01160 to be −77.59, −58.11, and −55.06 kcal/mol, respectively. A noteworthy finding is that a 4-methylpiperazino moiety occurred in all the three top hit compounds, since compounds possessing this moiety have recently been shown capable of inhibiting sphingosine 1-phosphate lyase,[55] and cyclin-dependent kinase 4 and AMPK-related kinase 5[56] by effectively binding to their active sites. Thus, the presence of the methylpiperazino group in all three hit compounds possibly contributed to enhanced binding efficiency and, therein, inhibition of the protease enzyme, calpain.

Protein−Ligand Complex Simulation. In order to validate the results of docking simulation, as well as to analyze the stability and interaction pattern of the hit compound, molecular dynamics simulations were performed. Only the HTS08688 complex, which showed the highest Glide score and binding energy, was taken for this purpose since it was to be used for further experimental analysis. Figure 4 shows the root-

DOI: 10.1021/acs.jcim.5b00092
J. Chem. Inf. Model. 2015, 55, 1686−1697

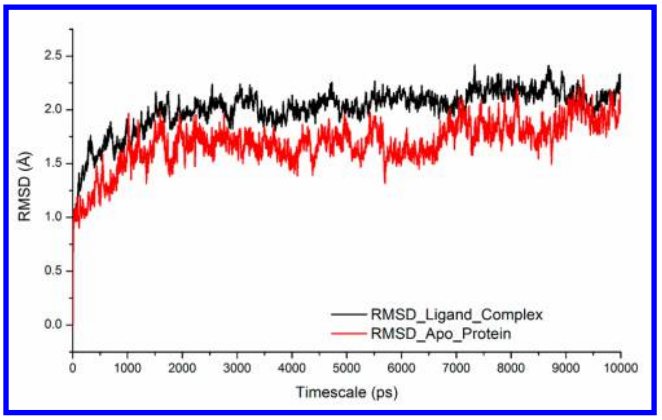

Figure 4. Comparative molecular dynamics analysis of 1KXR protein alone and the 1KXR–HTS08688 complex. RMSD values of the 1KXR–HTS08688 complex (black line) and 1KXR alone (red line) systems versus simulation time (10 000 ps). *X* and *Y* axes represent time (ps), and root mean square deviation (RMSD), respectively.

mean-square deviation of the HTS08688 complex following dynamics simulation for 10 ns. Analysis of trajectories revealed that the HTS08688 complex was stable and well within the binding pocket of calpain 1. The complex appears to have been stable mainly due to the strong hydrogen bond interaction and cation–π interaction with the active site residues Gln 109, Cys 115, Glu 261, His 272 and Trp 298. Although the cation–π interaction is noncovalent, it is equivalent to or stronger than, a hydrogen bond.[57] In the present investigation, two such cation–π interactions were found. One such interaction existed between the Trp 298 residue of calpain 1 and the piperazino moiety of HTS08688, possibly due to the π-system contributed by the aromatic side chain of Trp 298. The other cation–π interaction was noted between the His 272 residue and benzoyl group of HTS08688; in this interaction His272 possibly provided the cation and the ligand facilitated the formation of π-system, a concept stated by Zacharias and Dougherty.[57] HTS08688 also appeared to possess a "solid wedge" chiral bond between the methylpiperazino ring and the acetamide moiety. According to Singh et al.[58] chiral bonds are effective during lead optimization since they improve the selectivity of the target, and enhance the pharmacokinetics and reduce the toxicity of the compound. Several studies have highlighted the significance of chirality in drug designing. In one such study by Vassilev et al.[59] a crystal structure of human mouse double minute 2 protein (MDM2) complexed with a compound, nutulin-2, exhibiting racemic mixture, interacted effectively with MDM2 at the $_p$53 binding site, thereby preventing progression of a cancerous tumor.[60,61] Similarly, the macrocyclic calpain inhibitor (CAT811) described by Abell et al.[62] also possessed a chiral bond, and the presence of this chiral bond possibly enhanced the selective binding of CAT811 to calpain, thereby retarding calcium-induced opacification in in vitro cultured ovine lenses. Hence, it may be postulated that the chiral bond present in the hit compound HTS08688 possibly was instrumental in enhancing the stability of the protein–ligand interaction during molecular dynamics analysis.

EXPERIMENTAL VALIDATION

In order to ascertain the anticataractogenic potential of HTS08688 by virtue of its calpain inhibitory property, in the present investigation, an in vitro rat model of selenite-induced cataract was used.

In Vitro Phase of the Study. Gross assessment revealed that none of the eight rat lenses in group I (that had been incubated in DMEM alone) showed any opacification (grade 0) even after 24 h incubation (Table 2). However, all (100%)

Table 2. Morphological Assessment of Cultured Rat Lenses (in Vitro Study)

groups of lenses (incubated in DMEM)	total no. of lenses	morphology of lenses[a]	number of lenses exhibiting the morphology
group I (DMEM only)	8	0	all 8
group II (DMEM and selenite)	8	+++	all 8
group III (DMEM, selenite, HTS08688)	8	0	6 of 8
		+	2 of 8

[a]Degree of opacification: (0) absence of opacification; (+) slight degree of opacification; (++) moderate degree of opacification; (+++) extensive thick opacification involving the entire lens.

lenses in group II (that had been incubated in DMEM and selenite) showed total (grade +++) opacification after 24 h incubation. Interestingly, only two of eight lenses (25%) in group III (that had been incubated in DMEM with selenite and HTS08688 added simultaneously) revealed grade + opacification after 24 h incubation, while the remaining six (75%) lenses did not show any opacification at all (grade 0) (Table 2). Grade ++ opacification was not observed in any of the lenses. The difference between the proportion of opacified lenses (100%) in group II versus that (25%) in group III was found to be statistically significant (χ^2 [df = 1] = 8; $p < 0.05$) (Table 2, Figure 5). These results suggest that the addition of HTS08688 to the DMEM medium containing selenite, partially prevented the occurrence of lenticular opacification caused by exposure to selenite, possibly by inhibiting the calpain protein. The results of the current investigation corroborate those of an earlier

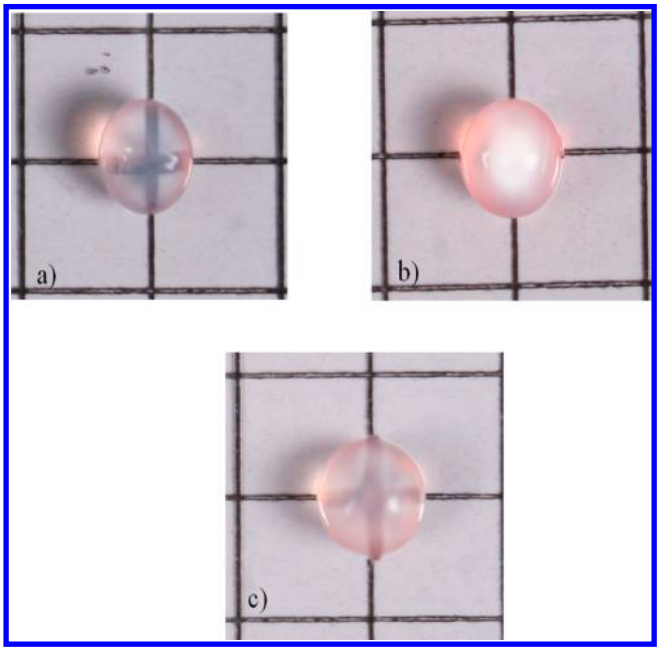

Figure 5. In vitro cultured Wistar rat lenses. (a) Group I lens (cultured in DMEM only). (b) Group II lens (cultured in DMEM and selenite). (c) Group III lens (cultured in DMEM + selenite + 100 μM/mL of HTS08688).

DOI: 10.1021/acs.jcim.5b00092
J. Chem. Inf. Model. 2015, 55, 1686–1697

Table 3. In Vitro Study: Activities of Antioxidant Enzymes and Redox Component in Wistar rat lenses cultured in Dulbecco's modified Eagle's medium[a]

Activity of Antioxidant Enzymes in Cultured Lenses			
enzymes (unit of activity)	group I (normal)	group II (selenite-challenged, untreated)	group III (selenite-challenged, HTS08688-treated)
superoxide dismutase (unit/min·mg protein)	2.85 ± 0.53	1.97 ± 0.25[b]	2.60 ± 0.32[c]
catalase (mmol H_2O_2 consumed/min·mg protein)	7.11 ± 0.72	4.42 ± 0.48[b]	5.87 ± 0.63[c]
glutathione peroxidase (μmol glutathione oxidized/min·mg protein)	34.96 ± 0.95	26.85 ± 0.76[b]	32.51 ± 0.87[c]
Activity of Redox Component System in Cultured Lenses			
component analyzed (unit of activity)	group I (normal)	group II (selenite-challenged, untreated)	group III (selenite-challenged, HTS08688-treated)
reduced glutathione (μmol/g wet weight of lens)	8.84 ± 0.43	3.83 ± 0.40[b]	6.48 ± 0.35[c]

[a]All values are expressed as mean ± SD of six determinations. [b]Statistically significant difference ($P < 0.05$) when compared with both group I and III values. [c]Statistically significant difference ($P < 0.05$) when compared with group II values.

study by Jones et al.,[63] wherein the selective calpain inhibitor, CAT0059, protected the lens from opacification in an in vitro ovine lens culture system.

Quantitative Analysis of Biochemical Parameters. In order to delineate the putative mechanisms by which HTS08688 retarded the progression of selenite-induced cataract, the status of enzymatic and nonenzymatic antioxidants and rate of lipid peroxidation were determined. When experimental animals are challenged with selenite, there is enhanced lenticular lipid peroxidation and formation H_2O_2 within the aqueous humor of the eye.[64] Selenite has also been found to reduce lenticular GSH levels,[64] possibly because the reaction of selenite with GSH leads to the generation of active oxygen.[65] So also, in the present investigation, lower mean activities of CAT, SOD, GPx and GSH were detected in group II rats lenses (incubated in DMEM containing selenite only) than those in group I rat lenses, which had been incubated in DMEM alone. However, the mean activities of CAT, SOD, GPx, and GSH in group III rat lenses (that had been incubated in DMEM containing selenite and the calpain inhibitor-HTS08688) were found to be significantly higher than those occurring in group II rat lenses (Table 3). The basic mechanism by which free radicals damage cells is considered to be accelerated by lipid peroxidation;[66] oxidative stress is characterized by enhanced lipid peroxidation, which manifests as a rise in the level of MDA. However, in the current investigation, the mean concentration of MDA was significantly lower in group III rat lenses (treated with HTS08688) than that in group II rat lenses and approximated the normal levels of group I rat lenses (Table 4).

Table 4. In Vitro Study: Levels of Malondialdehyde in Wistar Rat Lenses Cultured in Dulbecco's Modified Eagle's Medium[a]

lipid peroxidation (unit of activity)	group I (normal)	group II (selenite-challenged, untreated)	group III (selenite-challenged, HTS08688-treated)
MDA (nmol/g wet weight of lens)	62.66 ± 0.69	82.73 ± 0.79[b]	71.29 ± 0.86[c]

[a]All values are expressed as mean ± SD of six determinations. [b]Statistically significant difference ($P < 0.05$) when compared with both group I and III values. [c]Statistically significant difference ($P < 0.05$) when compared with group II values.

It has long been stated that augmentation of the antioxidant defense of the lens may prevent or delay experimental cataracts.[2] The data obtained from the current investigation suggest that HTS08688 partially prevents the sudden decline in lenticular antioxidant enzyme activities that follow exposure of rat lenses to sodium selenite; this evasive effect was demonstrated morphologically by a decrease in the intensity of lenticular opacification. Recently, Ölgen et al.[67] demonstrated that acetamide derivatives exhibit antioxidant property; HTS08688 also possesses an acetamide moiety attached to its functional group. Hence, in the present study, maintenance of antioxidant defenses at near normal values in the HTS08688-treated group of rat lenses was possibly due to the presence of this acetamide group. Our results are consistent with those reported by others wherein known antioxidants have been tested for anticataractogenic potential.[68,69]

Cytochemical Localization. The superoxide radical, O_2^-, is considered toxic to cellular components, as it acts as a precursor of reactive oxygen species.[70] Selenite administration leads to a marked increase in lenticular SOD-inhibitable O_2^- generation, suggesting that selenium-induced generation of free radicals may contribute to progression of oxidative stress and cataractogenesis.[71,72] NBT staining serves as a heuristic approach for localizing superoxide generation in the ocular lens. NBT, on reacting with superoxide, forms dark-blue insoluble formazan crystals.[73] In the present study, intense blue deposits of formazan were shown by cytochemical localization in the lenses of group II (selenite-challenged, untreated) rats, suggesting O_2^- generation (Figure 6b). However, group III rat lenses (selenite-challenged, HTS08688-treated) exhibited negligible formazan deposition (Figure 6c), and the pattern was similar to that of group I (normal) lenses (Figure 6a). These results also suggest the antioxidative potential of HTS08688.

Calcium Level and Calpain Activity. Biswas et al.[8] suggest that certain types of cataract, both in animals and humans, are an outcome of unregulated calcium-mediated proteolysis of key lenticular proteins by calpains. Furthermore, Lee et al.[74] demonstrated the impact of calcium overload and subsequent activation of calpain in cultured ovine lens. Hence, in the present investigation, we have attempted to determine the calcium concentration among the experimental groups of rat lenses. It was noted that the mean calcium concentration was significantly higher in group II (selenite-challenged, untreated) rat lenses than that in group III (selenite-challenged, HTS08688-treated) and group I (normal) rat lenses (Figure 7).

DOI: 10.1021/acs.jcim.5b00092
J. Chem. Inf. Model. 2015, 55, 1686−1697

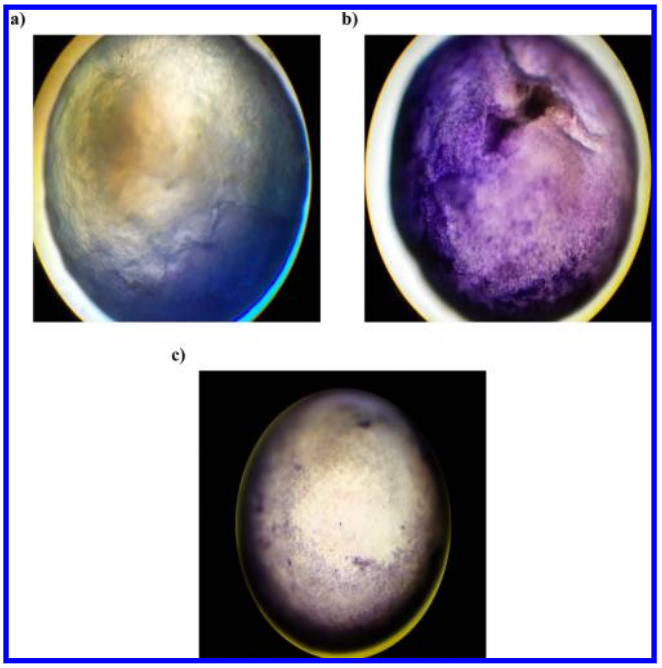

Figure 6. Cytochemical localization of nitroblue tetrazolium-reducing substances in in vitro cultured Wistar rat lenses. (a) Group I (normal) formazon crystal not formed. (b) Group II (selenite-challenged, untreated) formazon crystal formed. (c) Group III (selenite-challenged, HTS08688-treated) formazon crystal formation prevented.

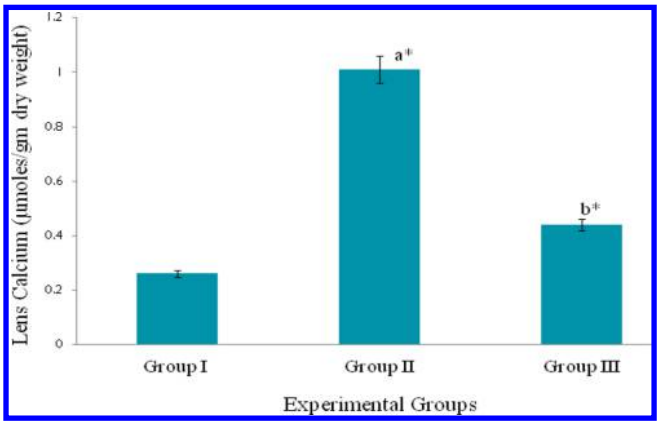

Figure 7. Mean calcium levels in in vitro cultured lenses of Wistar rats: group I (normal), group II (selenite-challenged, untreated), and group III (selenite-challenged, HTS08688 treated). The mean calcium level in group II rat lenses was higher than that in normal and that in HTS08688-treated rat lenses. Values are expressed as mean ± SD. (a*) Group II vs I ($P < 0.05$). (b*) Group III vs II ($P < 0.05$).

The demonstrated higher level of lenticular calcium was possibly due to oxidation of sulfhydryl groups or changes in the membrane polarity caused due to lipid peroxidation by selenite. However, treatment with HTS08688 prevented such changes possibly by preventing selenite-induced oxidative insults; in addition the presence of a chiral bond to the nitrogen atom of the methylpiperazino ring of HTS08688 may have prevented a sudden increase in the calcium level in the rat lenses. Li et al.[75] made a similar observation with the CPU 86017 compound; a chiral center located at the nitrogen atom of CPU 86017 was reported to play a key role in blocking calcium influx, thereby maintaining the ionic homeostasis and enhancing its antiarrhythmic potential in the aorta.

Shearer et al.[6] were of the opinion that the loss of Ca^{2+}-ATPase activity may be attributed to the oxidative stress-mediated lipid peroxidative damage on lenticular membranes, leading to influx of calcium. This elevated calcium leads to the activation of lenticular calpains, thereby resulting in proteolysis of lenticular crystallins. Hence, in the current investigation, an effort was made to measure the calpain activity in lenses of the experimental groups. Decreased calpain activity was observed in the rat lenses that were selenite-challenged, untreated (group II). However, such a decline in this activity was prevented in group III (selenite-challenged, calpain inhibitor-HTS08688-treated) lenses, and the level approximated normal levels (Figure 8). Decreased lenticular calpain activity appeared to

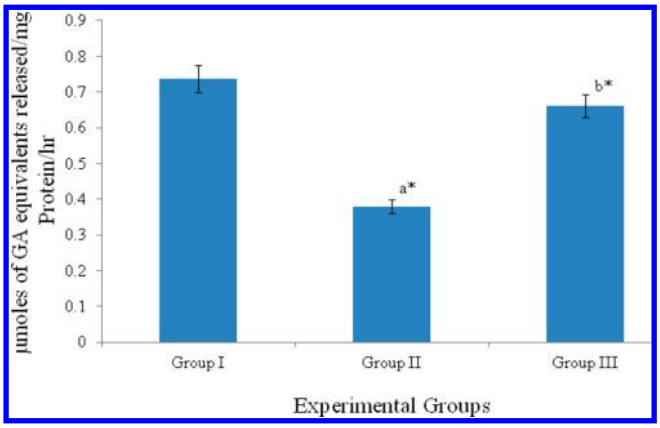

Figure 8. Mean calpain activity in in vitro cultured lenses of Wistar rats: group I = normal, group II = selenite-challenged, untreated, group III = selenite-challenged, HTS08688-treated, GA = glutamic acid. Values are expressed as mean ± SD. (a*) Group II vs I ($P < 0.05$). (b*) Group III vs II ($P < 0.05$).

occur concomitantly with increased lenticular calcium levels, presumably due to the well-known autolysis of calpain that results from exposure of the enzyme to an elevated calcium concentration.[76]

Lens Histoarchitecture. Sectioning of lenticular tissues was performed to obtain further insight into a putative modulatory role of HTS08688 in maintaining the structural integrity of lenticular epithelial cells, which act as a primary line of defense against the oxidative insults. The histoarchitecture of the lenticular tissue in the experimental groups is shown in Figure 9a–c. Epithelial cells covered by a capsular layer were noted in the normal untreated (group I) rat lenses (Figure 9a). Lack of an intact capsule, degenerated epithelial cells, and fiber vacuolation were noted in the lenticular tissue of selenite-challenged, untreated (group II) rat lenses (Figure 9b). Interestingly, such alterations were prevented and almost normal structural integrity was maintained in rat lenses that had been treated with the calpain inhibitor-HTS08688 (Figure 9c). The results suggest that HTS08688 is capable of maintaining the structural integrity of lenticular epithelial cells, apparently ensuring a balanced ionic homeostasis.

Potential Cytotoxicity of HTS08688 in HLE-B3 Cells. In a noteworthy study by Worgul et al.,[77] it was stated that abnormal proliferation of lenticular epithelial cells to fiber cells leads to the formation of cataract. HLE-B3 cells maintain a normal differentiation of epithelial cells and serve as a platform for delineating the mechanism of cataractogenesis and to identify anticataract agents.[78] Hence, in the present investigation, we sought to determine the potential cytotoxicity of

DOI: 10.1021/acs.jcim.5b00092
J. Chem. Inf. Model. 2015, 55, 1686–1697

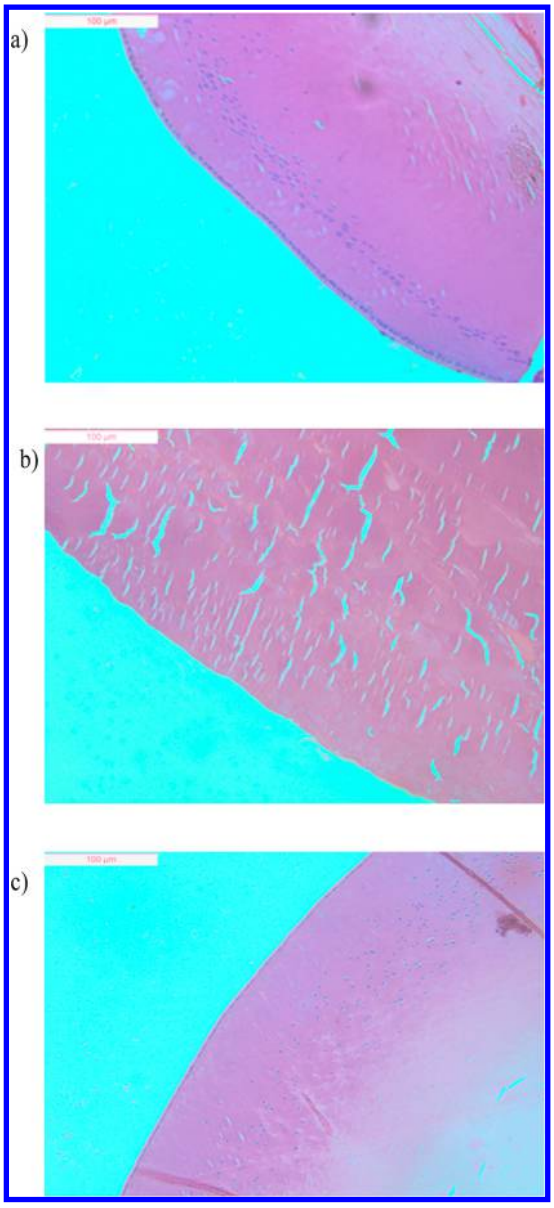

Figure 9. Histoarchitecture of in vitro cultured lenticular tissues of Wistar rats. Hematoxylin-eosin staining. ×100 magnification. (a) Normal untreated (group I) lenses showing beaded epithelial cells. (b) Selenite-challenged, untreated (group II) lenses showing degraded epithelial layer and severe vacuolation of the fiber cells at the cortex region. (c) Selenite-challenged, HTS08688-treated (group III) lenses showing preservation of almost normal profile of the epithelial cells and minimal vacuolation of fiber cells.

HTS08688 on HLE-B3 cells (Figure 10a), using an MTT assay. As illustrated in Figure 10b, HLE-B3 cells were treated with varying concentrations of HTS08688 (10−700 μM/mL) for 24 h. HTS08688 exhibited significant dose-dependent cytotoxicity ($p < 0.05$), with an IC_{50} value of 177 μM/mL at the end of the 24 h treatment period. There was a remarkable decrease in viability of cells exposed to concentrations greater than 300 μM/mL. These results suggest that the screened calpain inhibitor, HTS08688, is not toxic to human lenticular epithelial cells, thereby ensuring potential application for preventing/retarding cataractogenesis in humans. However, the data need to be extrapolated in order to identify the effective

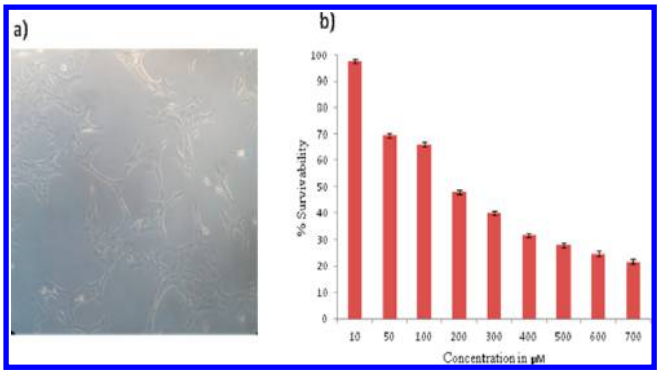

Figure 10. Cytotoxic potential of HTS08688 determined by reduction of tetrazolium salt 3-(4,5-(dimethyl-thyazol-2-yl)-2,5-diphenyl-tetrazolium (MTT). (a) Cultured human lens epithelial cells (HLE-B3). (b) Graph representing various concentrations of "Hit compound-HTS08688" and their corresponding percentage survivability.

concentration that would prevent degradation of lenticular crystallins.

CONCLUSION

In conclusion, the present investigation has created a novel paradigm in identifying a putative calpain inhibitor, HTS08688, through a synergistic approach of structure-based virtual screening and molecular dynamics simulation of the "protein−hit" complex. Furthermore, the efficacy of this hit compound, HTS08688, in preventing/retarding cataractogenesis was evaluated through an in vitro explant culture of rat lenses. The results obtained strongly suggest that the in silico-screened calpain inhibitor, HTS08688, dampens the cascade of events that follows selenite-induced calpain activation in Wistar rat lenses, therein preventing cataractogenesis. However, this hypothesis warrants further in-depth molecular investigations and clinical trials prior to using the hit compound in the pharmacological management of cataract.

Taken together, the results of this study highlight the significance of computational approaches, compared to the rational drug discovery process, in identifying potent inhibitors of calpain.

AUTHOR INFORMATION

Corresponding Author

*Fax: +91-431-2414969. E-mail: gerryarchup@yahoo.co.in.

Notes

The authors declare no competing financial interest.

ACKNOWLEDGMENTS

Financial support rendered by Council of Scientific & Industrial Research (CSIR), New Delhi, in the form of Senior Research Fellowship to the first author is thankfully acknowledged (ref no. 09/475 (0185)/2012-EMR-I). Financial support rendered by University Grants Commission-Basic Scientific Research (UGC-BSR) to the corresponding author is gratefully acknowledged. The authors immensely thank Dr. Sreedhar Rao (Centre for Cellular and Molecular Biology, Hyderabad, India) and Dr. D. Balasubramaniam (LV. Prasad Eye Institute, Hyderabad, India) for their kind gift of HLE-B3 cells and for their valuable suggestions in standardizing the culture conditions. The instrumentation facility provided by the University Grants Commission-Special Assistance Program (UGC-SAP-DRS-II)

DOI: 10.1021/acs.jcim.5b00092
J. Chem. Inf. Model. 2015, 55, 1686−1697

of the Department of Animal Science, Bharathidasan University, is also acknowledged.

REFERENCES

(1) Chang, D. F.; Braga-Mele, R.; Mamalis, N.; Masket, S.; Miller, K. M.; Nichamin, L. D.; Packard, R. B.; Packer, M. Prophylaxis of Postoperative Endophthalmitis After Cataract Surgery: Results of the 2007 ASCRS Member Survey. *J. Cataract Refractive Surg.* **2007**, *33*, 1801−1805.
(2) Spector, A. Oxidative Stress-Induced Cataract: Mechanism of Action. *FASEB. J.* **1995**, *9*, 1173−1182.
(3) Missiaen, L.; Callewaert, G.; Parys, J. B.; Wuytack, F.; Raeymaekers, L.; Droogmans, G.; Nilius, B.; Eggermont, J.; De Smedt, H. [Intracellular Calcium: Physiology and Physiopathology]. *Verh. K. Acad. Geneeskd. Belg.* **2000**, *62*, 471−499.
(4) Rhodes, J. D.; Sanderson, J. The Mechanisms of Calcium Homeostasis and Signalling in the Lens. *Exp. Eye Res.* **2009**, *88*, 226−234.
(5) Jedziniak, J. A.; Nicoli, D. F.; Yates, E. M.; Benedek, G. B. On the Calcium Concentration of Cataractous and Normal Human Lenses and Protein Fractions of Cataractous Lenses. *Exp. Eye Res.* **1976**, *23*, 325−332.
(6) Shearer, T. R.; Ma, H.; Fukiage, C.; Azuma, M. Selenite Nuclear Cataract: Review of the Model. *Mol. Vis.* **1997**, *3*, 8.
(7) Goll, D. E.; Thompson, V. F.; Li, H.; Wei, W.; Cong, J. The Calpain System. *Physiol. Rev.* **2003**, *83*, 731−801.
(8) Biswas, S.; Harris, F.; Dennison, S.; Singh, J.; Phoenix, D. A. Calpains: Targets of Cataract Prevention? *Trends Mol. Med.* **2004**, *10*, 78−84.
(9) Huang, Y.; Wang, K. K. The Calpain Family and Human Disease. *Trends Mol. Med.* **2001**, *7*, 355−362.
(10) Shearer, T. R.; Ma, H.; Shih, M.; Fukiage, C.; Azuma, M. Calpains in the Lens and Cataractogenesis. *Methods Mol. Biol.* **2000**, *144*, 277−285.
(11) Ray, S. K.; Hogan, E. L.; Banik, N. L. Calpain in the Pathophysiology of Spinal Cord Injury: Neuroprotection with Calpain Inhibitors. *Brain Res. Rev.* **2003**, *42*, 169−185.
(12) Sakamoto-Mizutani, K.; Fukiage, C.; Tamada, Y.; Azuma, M.; Shearer, T. R. Contribution of Ubiquitous Calpains to Cataracto-genesis in the Spontaneous Diabetic Wbn/Kob Rat. *Exp. Eye Res.* **2002**, *75*, 611−617.
(13) Takeuchi, N.; Ito, H.; Namiki, K.; Kamei, A. Effect of Calpain on Hereditary Cataractous Rat, ICR/f. *Biol. Pharm. Bull.* **2001**, *24*, 1246−1251.
(14) Elanchezhian, R.; Sakthivel, M.; Geraldine, P.; Thomas, P. A. The Effect of Acetyl-L-Carnitine on Lenticular Calpain Activity in Prevention of Selenite-Induced Cataractogenesis. *Exp. Eye Res.* **2009**, *88*, 938−944.
(15) Payne, R. J.; Brown, K. M.; Coxon, J. M.; Morton, J. D.; Lee, H. Y.; Abell, A. D. Peptidic Aldehydes Based on α- and β-Amino Acids: Synthesis, Inhibition of m-Calpain, and Anti-Cataract Properties. *Aust. J. Chem.* **2004**, *57*, 877−884.
(16) Stuart, B. G.; Coxon, J. M.; Morton, J. D.; Abell, A. D.; McDonald, D. Q.; Aitken, S. G.; Jones, M. A.; Bickerstaffe, R. Molecular Modeling: A Search for a Calpain Inhibitor as a New Treatment for Cataractogenesis. *J. Med. Chem.* **2011**, *54*, 7503−7522.
(17) Donkor, I. O. A Survey of Calpain Inhibitors. *Curr. Med. Chem.* **2000**, *7*, 1171−1188.
(18) Lubisch, W.; Moeller, A. Discovery of Phenyl Alanine Derived Ketoamides Carrying Benzoyl Residues as Novel Calpain Inhibitors. *Bioorg. Med. Chem. Lett.* **2002**, *12*, 1335−1338.
(19) *Maestro*, version 9.2; Schrödinger LLC: New York, USA, 2011.
(20) Moldoveanu, T.; Hosfield, C. M.; Lim, D.; Elce, J. S.; Jia, Z.; Davies, P. L. A Ca(2+) Switch Aligns the Active Site of Calpain. *Cell* **2002**, *108*, 649−660.
(21) Berman, H. M.; Battistuz, T.; Bhat, T. N.; Bluhm, W. F.; Bourne, P. E.; Burkhardt, K.; Feng, Z.; Gilliland, G. L.; Iype, L.; Jain, S.; Fagan, P.; Marvin, J.; Padilla, D.; Ravichandran, V.; Schneider, B.; Thanki, N.; Weissig, H.; Westbrook, J. D.; Zardecki, C. The Protein Data Bank. *Acta Crystallogr., Sect. D: Biol. Crystallogr.* **2002**, *58*, 899−907.
(22) *MacroModel*, version 9.9.1; Schrödinger LLC: New York, USA, 2011.
(23) *Epik*, version 2.3; Schrödinger LLC: New York, USA, 2011.
(24) Muralidharan, A. R.; Selvaraj, C.; Singh, S.; Nelson Jesudasan, C. A.; Geraldine, P.; Thomas, P. Virtual Screening Based on Pharmacophoric Features of Known Calpain Inhibitors to Identify Potent Inhibitors of Calpain. *Med. Chem. Res.* **2014**, *23*, 2445−2455.
(25) *Impact*, version 5.8; Schrödinger LLC: New York, USA, 2011.
(26) *Prime*, version 3.1; Schrödinger LLC: New York, USA, 2011.
(27) Halgren, T. New Method for Fast and Accurate Binding-Site Identification and Analysis. *Chem. Biol. Drug Des.* **2007**, *69*, 146−148.
(28) *Sitemap*, version 2.5; Schrödinger LLC: New York, USA, 2011.
(29) *LigPrep*, version 2.4; Schrödinger LLC: New York, USA, 2011.
(30) *Qikprop*, version 3.2; Schrödinger LLC: New York, USA, 2011.
(31) Lipinski, C. A.; Lombardo, F.; Dominy, B. W.; Feeney, P. J. Experimental and Computational Approaches to Estimate Solubility and Permeability in Drug Discovery and Development Settings. *Adv. Drug Delivery Rev.* **2001**, *46*, 3−26.
(32) Friesner, R. A.; Murphy, R. B.; Repasky, M. P.; Frye, L. L.; Greenwood, J. R.; Halgren, T. A.; Sanschagrin, P. C.; Mainz, D. T. Extra Precision Glide: Docking and Scoring Incorporating a Model of Hydrophobic Enclosure for Protein-Ligand Complexes. *J. Med. Chem.* **2006**, *49*, 6177−6196.
(33) Selvaraj, C.; Sivakamavalli, J.; Vaseeharan, B.; Singh, P.; Singh, S. K. Structural Elucidation of srta Enzyme in Enterococcus Faecalis: An Emphasis on Screening of Potential Inhibitors Against the Biofilm Formation. *Mol. BioSyst.* **2014**, *10*, 1775−1789.
(34) Mobley, D. L.; Dill, K. A. Binding of Small-Molecule Ligands to Proteins: "What You See" is not Always "What You Get". *Structure* **2009**, *17*, 489−498.
(35) Klepeis, J. L.; Lindorff-Larsen, K.; Dror, R. O.; Shaw, D. E. Long-Timescale Molecular Dynamics Simulations of Protein Structure And Function. *Curr. Opin. Struct. Biol.* **2009**, *19*, 120−127.
(36) Shivakumar, D.; Harder, E.; Damm, W.; Friesner, R. A.; Sherman, W. Improving the Prediction of Absolute Solvation Free Energies using the Next Generation OPLS Force Field. *J. Chem. Theory Comput.* **2012**, *8*, 2553−2558.
(37) Bradford, M. M. A Rapid and Sensitive Method for the Quantitation of Microgram Quantities of Protein Utilizing the Principle of Protein-Dye Binding. *Anal. Biochem.* **1976**, *72*, 248−254.
(38) Marklund, S.; Marklund, G. Involvement of the Superoxide Anion Radical in the Autoxidation of Pyrogallol and a Convenient Assay for Superoxide Dismutase. *Eur. J. Biochem.* **1974**, *47*, 469−474.
(39) Sinha, A. K. Colorimetric Assay of Catalase. *Anal. Biochem.* **1972**, *47*, 389−394.
(40) Rotruck, J. T.; Pope, A. L.; Ganther, H. E.; Swanson, A. B.; Hafeman, D. G.; Hoekstra, W. G. Selenium: Biochemical Role as a Component of Glutathione Peroxidase. *Science* **1973**, *179*, 588−590.
(41) Moron, M. S.; Depierre, J. W.; Mannervik, B. Levels of Glutathione, Glutathione Reductase and Glutathione S-Transferase Activities in Rat Lung and Liver. *Biochim. Biophys. Acta, Gen. Subj.* **1979**, *582*, 67−78.
(42) Ohkawa, H.; Ohishi, N.; Yagi, K. Assay for Lipid Peroxides in Animal Tissues by Thiobarbituric Acid Reaction. *Anal. Biochem.* **1979**, *95*, 351−358.
(43) Zhang, H.; Agardh, E.; Agardh, C. D. Nitro Blue Tetrazolium Staining: A Morphological Demonstration of Superoxide in the Rat Retina. *Graefe's Arch. Clin. Exp. Ophthalmol.* **1993**, *231*, 178−183.
(44) Banay-Schwartz, M.; DeGuzman, T.; Faludi, G.; Lajtha, A.; Palkovits, M. Alteration of Protease Levels in Different Brain Areas of Suicide Victims. *Neurochem. Res.* **1998**, *23*, 953−959.
(45) Nakai, N.; Lai, C. Y.; Horecker, B. L. Use of Fluorescamine in the Chromatographic Analysis of Peptides from Proteins. *Anal. Biochem.* **1974**, *58*, 563−570.
(46) Sisk, D. R.; Kuwabara, T. Histologic Changes in the Inner Retina of Albino Rats Following Intravitreal Injection of Monosodium

DOI: 10.1021/acs.jcim.5b00092
J. Chem. Inf. Model. 2015, 55, 1686−1697

L-Glutamate. *Graefe's Arch. Clin. Exp. Ophthalmol.* **1985**, *223*, 250−258.
(47) Andersson, M.; Sjostrand, J.; Andersson, A. K.; Andersen, B.; Karlsson, J. O. Calpains in Lens Epithelium from Patients with Cataract. *Exp. Eye Res.* **1994**, *59*, 359−364.
(48) Thampi, P.; Hassan, A.; Smith, J. B.; Abraham, E. C. Enhanced C-Terminal Truncation of αa- and αb-Crystallins in Diabetic Lenses. *Invest. Ophthalmol. Vis. Sci.* **2002**, *43*, 3265−3272.
(49) Moldoveanu, T.; Hosfield, C. M.; Lim, D.; Jia, Z.; Davies, P. L. Calpain Silencing by a Reversible Intrinsic Mechanism. *Nat. Struct. Biol.* **2003**, *10*, 371−378.
(50) Shoichet, B. K. Virtual Screening of Chemical Libraries. *Nature* **2004**, *432*, 862−865.
(51) Cheng, T.; Li, Q.; Zhou, Z.; Wang, Y.; Bryant, S. H. Structure-Based Virtual Screening for Drug Discovery: A Problem-Centric Review. *AAPS J.* **2012**, *14*, 133−141.
(52) Ghosh, S.; Nie, A.; An, J.; Huang, Z. Structure-Based Virtual Screening of Chemical Libraries for Drug Discovery. *Curr. Opin. Chem. Biol.* **2006**, *10*, 194−202.
(53) Perola, E.; Walters, W. P.; Charifson, P. S. A Detailed Comparison of Current Docking and Scoring Methods on Systems of Pharmaceutical Relevance. *Proteins: Struct., Funct., Genet.* **2004**, *56*, 235−249.
(54) Powers, J. C.; Asgian, J. L.; Ekici, O. D.; James, K. E. Irreversible Inhibitors of Serine, Cysteine, and Threonine Proteases. *Chem. Rev.* **2002**, *102*, 4639−4750.
(55) Weiler, S.; Braendlin, N.; Beerli, C.; Bergsdorf, C.; Schubart, A.; Srinivas, H.; Oberhauser, B.; Billich, A. Orally Active 7-Substituted (4-Benzylphthalazin-1-Yl)-2-Methylpiperazin-1-Yl] Nicotinonitriles as Active-Site Inhibitors of Sphingosine 1-Phosphate Lyase for the Treatment of Multiple Sclerosis. *J. Med. Chem.* **2014**, *57*, 5074−5084.
(56) Reddy, M. V.; Akula, B.; Cosenza, S. C.; Athuluridivakar, S.; Mallireddigari, M. R.; Pallela, V. R.; Billa, V. K.; Subbaiah, D. R.; Bharathi, E. V.; Vasquez-Del Carpio, R.; Padgaonkar, A.; Baker, S. J.; Reddy, E. P. Discovery of 8-Cyclopentyl-2-[4-(4-methyl-piperazin-1-yl)-Phenylamino]-7-Oxo-7,8-Dihydro-Pyrid o[2,3-d]Pyrimidine-6-Carbonitrile (7x) as a Potent Inhibitor of Cyclin-Dependent Kinase 4 (CDK4) and AMPK-Related Kinase 5 (ARK5). *J. Med. Chem.* **2014**, *57*, 578−599.
(57) Zacharias, N.; Dougherty, D. A. Cation-pi Interactions in Ligand Recognition And Catalysis. *Trends Pharmacol. Sci.* **2002**, *23*, 281−287.
(58) Singh, J.; Hagen, T. J.; Abraham, D. J. Chirality and Biological Activity. In *Burger's Medicinal Chemistry and Drug Discovery*; John Wiley & Sons, Inc., 2003; pp 127−166.
(59) Vassilev, L. T.; Vu, B. T.; Graves, B.; Carvajal, D.; Podlaski, F.; Filipovic, Z.; Kong, N.; Kammlott, U.; Lukacs, C.; Klein, C.; Fotouhi, N.; Liu, E. A. In Vivo Activation of the p53 Pathway by Small-Molecule Antagonists of MDM2. *Science* **2004**, *303*, 844−848.
(60) Lu, Y.; Nikolovska-Coleska, Z.; Fang, X.; Gao, W.; Shangary, S.; Qiu, S.; Qin, D.; Wang, S. Discovery of a Nanomolar Inhibitor of the Human Murine Double Minute 2 (MDM2)-p53 Interaction Through an Integrated, Virtual Database Screening Strategy. *J. Med. Chem.* **2006**, *49*, 3759−3762.
(61) Vassilev, L. T. MDM2 Inhibitors for Cancer Therapy. *Trends Mol. Med.* **2007**, *13*, 23−31.
(62) Abell, A. D.; Jones, M. A.; Coxon, J. M.; Morton, J. D.; Aitken, S. G.; McNabb, S. B.; Lee, H. Y.; Mehrtens, J. M.; Alexander, N. A.; Stuart, B. G.; Neffe, A. T.; Bickerstaffe, R. Molecular Modeling, Synthesis, and Biological Evaluation of Macrocyclic Calpain Inhibitors. *Angew. Chem., Int. Ed.* **2009**, *48*, 1455−1458.
(63) Jones, M. A.; Morton, J. D.; Coxon, J. M.; McNabb, S. B.; Lee, H. Y.; Aitken, S. G.; Mehrtens, J. M.; Robertson, L. J.; Neffe, A. T.; Miyamoto, S.; Bickerstaffe, R.; Gately, K.; Wood, J. M.; Abell, A. D. Synthesis, Biological Evaluation and Molecular Modelling of N-Heterocyclic Dipeptide Aldehydes as Selective Calpain Inhibitors. *Bioorg. Med. Chem.* **2008**, *16*, 6911−6923.
(64) David, L. L.; Shearer, T. R. State of Sulfhydryl in Selenite Cataract. *Toxicol. Appl. Pharmacol.* **1984**, *74*, 109−115.
(65) Seko, Y.; Saito, Y.; Kitahara, J.; Imura, N. Active Oxygen Generation by the Reaction of Selenite with Reduced Glutathione In Vitro. In *Selenium in Biology and Medicine*; Wendel, A., Ed.; Springer: Berlin, Heidelberg, 1989; pp 70−73.
(66) Esterbauer, H.; Schaur, R. J.; Zollner, H. Chemistry and Biochemistry of 4-Hydroxynonenal, Malonaldehyde and Related Aldehydes. *Free Radical Biol. Med.* **1991**, *11*, 81−128.
(67) Ölgen, S.; Bakar, F.; Aydin, S.; Nebioğlu, D.; Nebioğlu, S. Synthesis of New Indole-2-Carboxamide and 3-Acetamide Derivatives and Evaluation their Antioxidant Properties. *J. Enzyme Inhib. Med. Chem.* **2013**, *28*, 58−64.
(68) Geraldine, P.; Sneha, B. B.; Elanchezhian, R.; Ramesh, E.; Kalavathy, C. M.; Kaliamurthy, J.; Thomas, P. A. Prevention of Selenite-Induced Cataractogenesis by Acetyl-L-Carnitine: An Experimental Study. *Exp. Eye Res.* **2006**, *83*, 1340−1349.
(69) Isai, M.; Elanchezhian, R.; Sakthivel, M.; Chinnakkaruppan, A.; Rajamohan, M.; Jesudasan, C. N.; Thomas, P. A.; Geraldine, P. Anticataractogenic Effect of an Extract of the Oyster Mushroom, *Pleurotus ostreatus*, in an Experimental Animal Model. *Curr. Eye Res.* **2009**, *34*, 264−273.
(70) Nanjo, F.; Goto, K.; Seto, R.; Suzuki, M.; Sakai, M.; Hara, Y. Scavenging Effects of Tea Catechins and their Derivatives on 1,1-Diphenyl-2-Picrylhydrazyl Radical. *Free Radical Biol. Med.* **1996**, *21*, 895−902.
(71) Manikandan, R.; Thiagarajan, R.; Beulaja, S.; Sudhandiran, G.; Arumugam, M. Curcumin Prevents Free Radical-Mediated Cataractogenesis through Modulations in Lens Calcium. *Free Radical Biol. Med.* **2010**, *48*, 483−492.
(72) Anitha, T. S.; Muralidharan, A. R.; Annadurai, T.; Jesudasan, C. A.; Thomas, P. A.; Geraldine, P. Putative Free Radical-Scavenging Activity of an Extract of *Cineraria maritima* in Preventing Selenite-Induced Cataractogenesis in Wistar Rat Pups. *Mol. Vis.* **2013**, *16*, 2551−2560.
(73) Flohe, L.; Otting, F. Superoxide Dismutase Assays. *Methods Enzymol.* **1984**, *105*, 93−104.
(74) Lee, H. Y.; Morton, J. D.; Sanderson, J.; Bickerstaffe, R.; Robertson, L. J. The Involvement of Calpains in Opacification Induced by Ca^{2+}-Overload in Ovine Lens Culture. *Vet. Ophthalmol.* **2008**, *11*, 347−355.
(75) Li, N.; Yang, L.; Dai, D. Z.; Wang, Q. J.; Dai, Y. Chiral Separation of Racemate CPU86017, an Anti-Arrhythmic Agent, Produces Stereoisomers Possessing Favourable Ion Channel Blockade and Less Alpha-Adrenoceptor Antagonism. *Clin. Exp. Pharmacol. Physiol.* **2008**, *35*, 643−650.
(76) Suzuki, K. Calcium Activated Neutral Protease: Domain Structure and Activity Regulation. *Trends Biochem. Sci.* **1987**, *12*, 103−105.
(77) Worgul, B. V.; Merriam, G. R., Jr.; Medvedovsky, C. Cortical Cataract Development—an Expression of Primary Damage to the Lens Epithelium. *Lens Eye Toxic. Res.* **1989**, *6*, 559−571.
(78) Andley, U. P.; Rhim, J. S.; Chylack, L. T., Jr.; Fleming, T. P. Propagation and Immortalization of Human Lens Epithelial Cells in Culture. *Invest. Ophthalmol. Vis. Sci.* **1994**, *35*, 3094−3102.

DOI: 10.1021/acs.jcim.5b00092
J. Chem. Inf. Model. 2015, 55, 1686−1697